Available online at www.sciencedirect.com

ScienceDirect

Ceramics International 39 (2013) 9549–9556

CERAMICS INTERNATIONAL

www.elsevier.com/locate/ceramint

Effect of hafnium-incorporation on the microstructure and dielectric properties of cobalt ferrite ceramics

S. Wells, C.V. Ramana*

Department of Mechanical Engineering, University of Texas at El Paso, El Paso, TX 79968, USA

Received 22 April 2013; received in revised form 12 May 2013; accepted 17 May 2013
Available online 30 May 2013

Abstract

The effect of hafnium (Hf) incorporation on the crystal structure, surface morphology, chemical composition and dielectric properties of cobalt ferrite ($CoFe_2O_4$) is reported. Hafnium incorporated Co-ferrite ($CoFe_{2-x}Hf_xO_4$) ceramics were prepared by varying the Hf concentration in the range of $x=0.0$–0.2. X-ray diffraction (XRD) studies indicate that the $CoFe_{2-x}Hf_xO_4$ ceramics crystallize in inverse spinel change to structure similar to that of pure $CoFe_2O_4$. Hafnium incorporation induces lattice expansion leading to increased lattice constant from 8.374 Å for pure $CoFe_2O_4$ to 8.391 Å for the highest Hf concentration ($x=0.2$) in $CoFe_{2-x}Hf_xO_4$. Dielectric constant of $CoFe_{2-x}Hf_xO_4$ ceramics is also enhanced compared to pure $CoFe_2O_4$ due to the lattice distortion upon Hf incorporation. Improved dielectric properties of $CoFe_{2-x}Hf_xO_4$ ceramics compared to pure $CoFe_2O_4$ is attributed to the lattice distortion due to larger Hf-ions substituting for smaller Fe-ions associated structural changes with increased Hf concentration. Frequency variation of the dielectric constant shows the dispersion that can be modeled with a modified Debye's function, which considers the possibility of more than one ion, contributing to the relaxation.

Keywords: C. Dielectric properties; Cobalt ferrite; Hafnium incorporation; Crystal structure; Lattice expansion

1. Introduction

Ferrites have been the subject of numerous investigations for many years due to their scientific and technological applications in the fields of electronics, optoelectronics, magnetics, magneto-electronics, electrochemical science and technology and biotechnology [1–31]. These materials exhibit remarkable properties such as high saturation magnetization, large permeability at high frequency, and remarkably high electrical resistivity, which are attractive for electronics and magneto-electronics [8–10,12–24]. Recently, ferrite compounds have also drawn considerable attention for their potential application as electrode materials in Li-ion batteries and solid oxide fuel cells [23,24]. $NiFe_2O_4$, $CoFe_2O_4$ and $CuFe_2O_4$ were demonstrated to be potential candidates for cathode materials in lithium batteries [23,24].

Cobalt ferrite ($CoFe_2O_4$), which belongs to the family of ferrite ceramics, has been widely studied due to its high electromagnetic performance, excellent chemical stability, mechanical hardness, high coercivity, moderate saturation magnetization, and possible integration into biomedicine and drug delivery applications [27,31]. While the structure, electrical and dielectric properties play a key role in designing the magnetic, electronic, microwave and electrochemical devices, the properties and phenomena of Co ferrites are dependent on microstructure and chemistry, which in turn depend on the fabrication and synthesis processes [29–33]. For instance, the electrical properties of a Co ferrite at room temperature are dependent on the exact chemical composition, firing temperature (if any), reactive/processing atmosphere and on the ions that substitute Fe^{3+}/Fe^{2+} ions [32–34]. In $CoFe_2O_4$, the relatively large oxygen ions form face centered cubic (FCC) lattice. In this cubic close-packed structure two kind of interstitial sites occur, the tetrahedral (A) and the octahedral (B) sites which are surrounded by four and six oxygen ions, respectively [32–34]. The tetrahedral (A) sites are occupied by

*Corresponding author. Tel.: +1 9157478690.
E-mail address: rvchintalapalle@utep.edu (C.V. Ramana).

0272-8842/$ - see front matter © 2013 Elsevier Ltd and Techna Group S.r.l. All rights reserved.
http://dx.doi.org/10.1016/j.ceramint.2013.05.073

the Fe^{3+} ions and the octahedral (B) sites are occupied by the Co^{2+} and Fe^{3+}, in equal proportions. The angle A–O–B is closer to 180° than the angles B–O–B and A–O–A, and therefore, the AB pair (Fe–Fe) has a strong superexchange (antiferromagnetic) interaction [32–34].

Partial substitution of Fe^{3+} by rare earth ion in the spinel structure has been reported to lead to structural distortion [8,12,29] that induces strain and significantly modifies the electrical and dielectric properties. It has been reported that inclusion of Zn, Cu, Co and Cd in ferrites [29,35] leads to an increase in the dielectric constant due to the formation of excess Fe^{2+} which leads to increase in hopping of electrons between Fe^{2+} and Fe^{3+}. The goal of the present work is to study the effect of hafnium (Hf) incorporation on the structure, electrical and dielectric properties of Co ferrite. The obvious relevance of the work is to examine whether the dielectric constant of these materials can be enhanced compared to pure Co ferrite while retaining their insulating nature. To the best of our knowledge, there are no existing reports on the effect of Hf on the electrical and dielectric properties of Co ferrite. Therefore, such an investigation is expected to contribute significantly to our current understanding of ion substitution in Co ferrites. In addition, the reason for Hf incorporation can be understood and beneficial from the view point of the fact that the Hf-based ceramic materials exhibit outstanding chemical and thermal stability and excellent electrical properties coupled with high dielectric constant [36–40]. For instance, hafnium oxide (HfO_2) is a high temperature refractory material with excellent physical and chemical properties [36–40]. The outstanding chemical stability, electrical and mechanical properties, high dielectric constant, and wide band gap of HfO_2 makes it suitable for several industrial applications in the field of electronics, magneto-electronics, structural ceramics, and optoelectronics [36–40]. HfO_2 has been identified as one of the most promising materials for the nanoelectronics industry to replace SiO_2 because of its high dielectric constant and expected stability in contact with Si [38,39]. The work reported in this paper is, therefore, focused on the synthesis of $CoFe_{2-x}Hf_xO_4$ ceramic materials and evaluation of their structure, chemical characteristics and dielectric properties.

2. Experimental details

2.1. Synthesis

The Hf incorporated Co ferrite, namely $CoFe_{2-x}Hf_xO_4$, ceramic materials were prepared employing the conventional solid state chemical reaction method. The starting materials were 99.99% pure CoO, Fe_2O_3, and HfO_2. Powders of the starting materials were ground in a mortar and pestle for 1 h and the mixtures were heat treated in air at 1200 °C for 12 h. The powders were made into pellets and then sintered at 1250 °C in air for 12 h. The compositions of the ceramics were varied to obtain x in the range of 0.0–0.2. Specifically, $CoFe_{2-x}Hf_xO_4$ ceramics with six different compositions yielding x values of 0.00, 0.05, 0.075, 0.10, 0.15 and 0.20 were synthesized. The resulting ceramic materials were then used for further investigation to characterize the microstructure and dielectric properties as a function of Hf-concentration.

2.2. Characterization

The crystal structure of the materials synthesized was investigated using a Bruker D8 Discover X-ray diffractometer employing Cu Kα radiation of wavelength 1.5406 Å. Surface morphology and composition were examined by scanning electron microscopy (SEM) coupled with energy dispersive X-ray spectrometry (EDS) using a high-performance and high-resolution scanning electron microscope (Hitachi S-4800). Sample for SEM and EDS analysis was prepared by dispersing $CoFe_{2-x}Hf_xO_4$ ceramic on carbon tape which was pasted on Al grid. Surface imaging analysis was performed using probe electron beam operating at 15 kV. The secondary electrons generated from sample were used for imaging the surface. Dielectric measurements were carried out at room temperature employing a LCR meter.

3. Results and discussion

3.1. Crystal structure and phase identification

The pure Co ferrite synthesized and as received hafnia materials were characterized using XRD measurements. XRD pattern of pure Co ferrite ($CoFe_2O_4$) is shown in Fig. 1. The calculated pattern after the Rietveld refinement, which was carried out using the GSAS program [41] is also shown (Fig. 1). The weighted refined parameter (wrp) and the χ^2 (goodness of the fit) values of the fitting are as indicated. XRD data indicate that the synthesized $CoFe_2O_4$ material crystallizes in the inverse spinel phase without any impurity phase. The lattice constant determined from XRD is 8.374 Å, which agrees with that of the reported value for $CoFe_2O_4$. XRD data of as-received HfO_2 ceramic powder was used as calibration check for the $CoFe_{2-x}Hf_xO_4$ ceramics in terms of phase purity, homogeneity and secondary phase growth (if any). The crystal structure of HfO_2 is monoclinic with lattice parameters $a=5.1156$ Å, $b=5.1722$ Å and $c=5.2948$ Å.

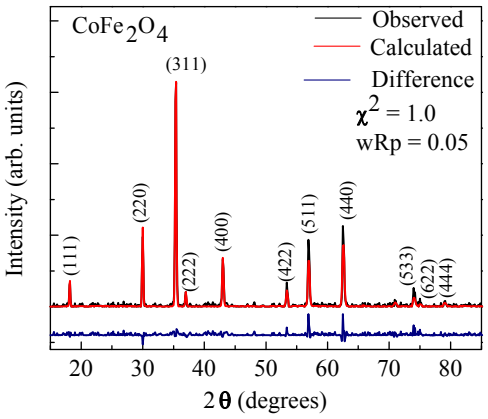

Fig. 1. XRD pattern of pure $CoFe_2O_4$. Indexing of the peaks is as shown. The calculated XRD pattern after the retvield refinement and the difference are also shown.

The crystal structure of the Hf-incorporated Co-ferrite ceramics showed interesting structural evolution as a function of HfO_2 content. The XRD patterns of the Hf-incorporated ferrites are shown in Fig. 2 as a function of Hf concentration ($x=0$–0.2). XRD patterns indicate that all the $CoFe_{2-x}Hf_xO_4$ ceramics also crystallize in inverse spinel phase, which is similar to that of pure $CoFe_2O_4$. However, formation of a small amount of HfO_2 phase was identified in substituted Co ferrites at higher Hf concentration. The lattice parameter values were obtained from XRD curves. The variation of lattice constant as a function of Hf concentration is shown in Fig. 3. Two important observations

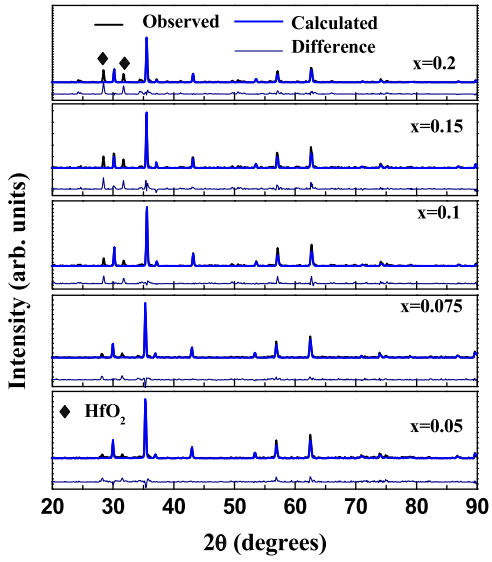

Fig. 2. XRD patterns of the $CoFe_{2-x}Hf_xO_4$ ceramics. The structural evolution with increasing Hf content is evident from the XRD data.

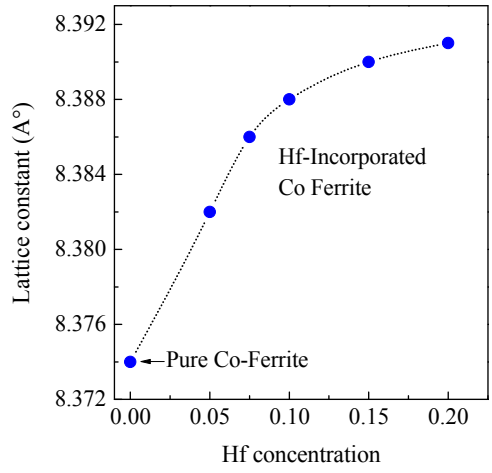

Fig. 3. Lattice constant variation with x values in $CoFe_{2-x}Hf_xO_4$ ceramics. It is evident that the lattice constant increases with increasing Hf concentration.

can be made from Fig. 3. Continuous increase in the lattice constant with progressive increase in Hf concentration is the first. The calculated lattice constant values for $CoFe_{2-x}Hf_xO_4$ ($x=0.00$, 0.05, 0.075, 0.10, 0.15 and 0.20) ceramics were found to increase from 8.374 Å to 8.391 Å. The lattice expansion is significant even for a very small amount of Hf ($x=0.05$) incorporation. The lattice constant determined for $x=0.05$ is 8.384 Å, which is a significant increase compared to that (8.374 Å) of pure $CoFe_2O_4$. The lattice expansion can be attributed to the ionic size difference in the Hf^{4+} ions compared to Fe^{3+} ions. The ionic size of Hf^{4+} (0.83 Å) is greater than that of Fe^{3+} (0.67 Å) and induces a lattice distortion upon Hf-incorporation of Fe lattice sites in $CoFe_2O_4$. The distortion in the lattice is evident from the changes in Fe–O–Fe, Hf–O–Fe, Hf–O–Co bond angles and bond lengths in the B site compared to pure $CoFe_2O_4$ [32,33] as presented in Table 1 for a specific composition of $x=0.05$.

3.2. Morphology and composition

The morphology of samples is represented in the SEM images shown in Fig. 4. It is evident that the crystallites are uniformly distributed. The presence of smooth grain boundaries can also be seen in the SEM image. The EDS measurements indicate that the grown materials are stoichiometric and homogeneous with a uniform distribution. The characteristic peaks of Fe, Co, Hf and O are evident in EDS of $CoFe_{2-x}Hf_xO_4$ shown in Fig. 5 as a function of Hf-concentration. X-ray energy is characteristic of generating atom and, therefore, detection of X-rays emitted provides the signature of the atoms present [41,42]. Therefore, EDS measurements can be used to qualitatively discuss the chemical quality of $CoFe_{2-x}Hf_xO_4$. The lines identified are Fe Kα, Co Kα, O Kα, and Co Lα at their respective energy positions, indicating that the X-rays are only due to Fe, Co, Hf and O present in the samples. X-ray lines from the Al grid and carbon tape can also be seen (Fig. 5), which is hard to eliminate but can be used as a reference. The absence of any other peaks except from Co, Fe, Hf, and O atoms indicate the $CoFe_{2-x}Hf_xO_4$ ceramics are synthesized with a good chemical quality, where no any elemental impurities are incorporated during chemical processing and/or handling. The peak intensity of Hf is found to be increasing with increasing of HfO_2 concentration as expected.

3.3. Dielectric properties

The frequency variation of the dielectric constant (ε') of Hf substituted Co ferrites are presented and compared with that of pure Co ferrite in Fig. 6. It can be seen (Fig. 6) that ε'

Table 1
Comparison of refined values of bond angle and bond length in pure $CoFe_2O_4$ and $CoFe_{1.95}Hf_{0.05}O_4$.

Compound	Fe^{3+}–O–Fe^{3+} (Hf^{4+}) bond angle (deg)	Co^{2+}–O–Co^{2+} bond angle (deg)	O–Fe^{3+} (Hf^{3+}) bond length (Å)
$CoFe_2O_4$	159.2	90.6	2.050
$CoFe_{1.95}Hf_{0.05}O_4$	157.2	90.1	2.184

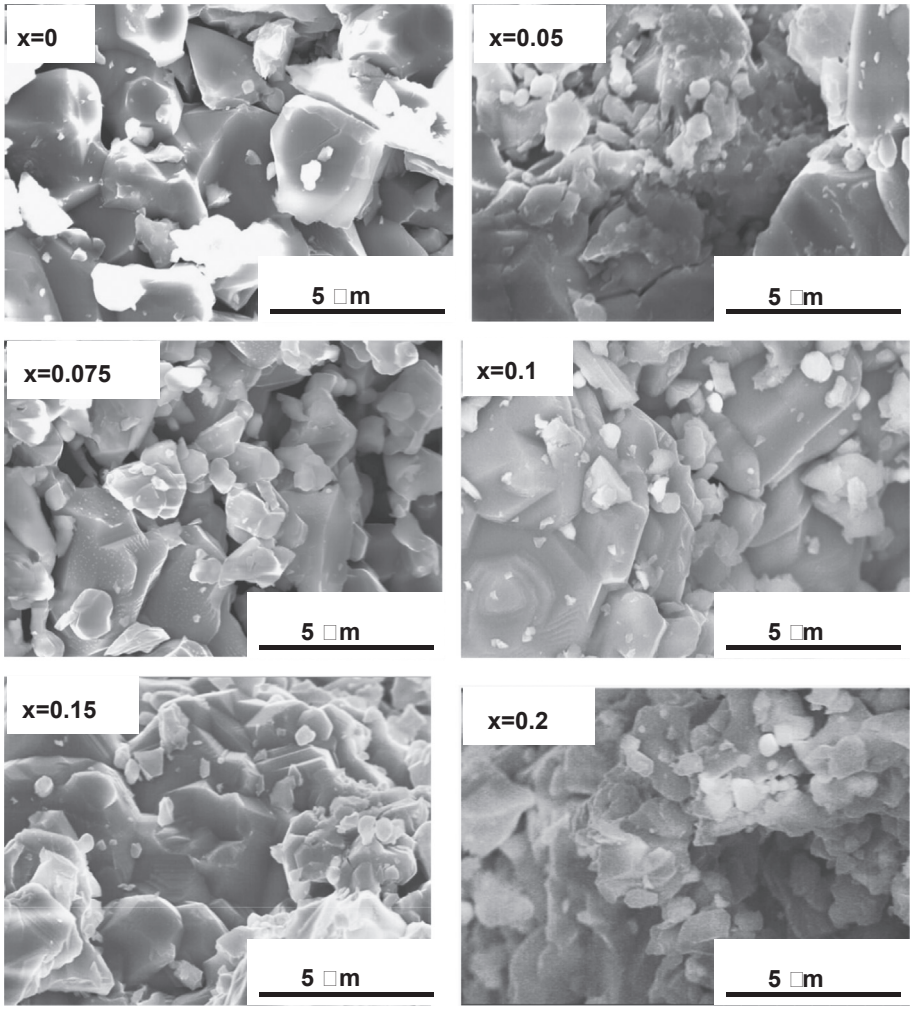

Fig. 4. SEM images of $CoFe_{2-x}Hf_xO_4$ ceramics as a function of x.

decreases with increasing frequency. The decrease of ε' with increasing frequency as observed for $CoFe_{2-x}Hf_xO_4$ materials is a typical dielectric behavior of spinel ferrites. At 100 Hz, ε' in Hf-substituted cobalt ferrites is in general higher than that of pure cobalt ferrite. In addition, ε' increases from 15.13×10^4 to 17.04×10^4 with increasing Hf concentration from $x=0.05$ to 2.00. The increase in the dielectric constant with the inclusion of Hf could be due to the fact that, with the inclusion of Hf, the Co ferrite lattice is distorted and increase in Fe (Hf)–O bond lengths at B site giving rise to increase in the atomic polarizability subsequently the dielectric constant. In addition, formation of small amounts of the respective HfO_2 phases at the grain boundaries leads to the accumulation of charges at the grain boundaries resulting in the interfacial polarization, which contributes to the additional increase in ε'. A decrease in ε' with increasing frequency is due to the fact the dipole lags behind the applied field at higher frequencies.

The dispersion of the real part of the dielectric constant can be explained based on the contributions from various sources of polarizations [43,44]. The larger value of ε' at lower frequencies, perhaps, could be due to all of the contributions (i.e, atomic, electronic, ionic, interfacial and grain-boundaries). The decrease (and disappearance finally) in ionic and orientation polarizability with increasing frequency may be responsible for the decrease in ε' at higher frequencies. Since more than one ion (O^{2-}, Hf^{4+} and Fe^{3+}) contributes to the relaxation process, the data were fit to the modified Debye's function, which takes the possibility of more than one ion contributing to the relaxation [33]. The observed dispersion of the dielectric constant can be modeled using the following equation [2]:

$$\varepsilon' - \varepsilon_\infty = \frac{(\varepsilon_0 - \varepsilon_\infty)}{[1 + (\omega\tau)^{2(1-\alpha)}]} \quad (1)$$

where ε' is the real part of the dielectric constant, ε_∞ is the dielectric constant at 1 MHz, τ is the mean relaxation time and α is the spreading factor of the actual relaxation times about the mean value. As seen in Fig. 6, the data fits well to such function implying that the relaxation process indeed is due to the multiple ions.

Following Debye model, an analysis of relaxation time for various compositions is made. It was found that this parameter increases with increasing Hf concentration in the ceramic. Mean relaxation time $\tau=0.309$ μs and $\alpha=0.43$ is obtained for pure Co ferrite. τ is found to increase from 0.432 μs to 0.444 μs with increasing Hf concentration from $x=0.05$

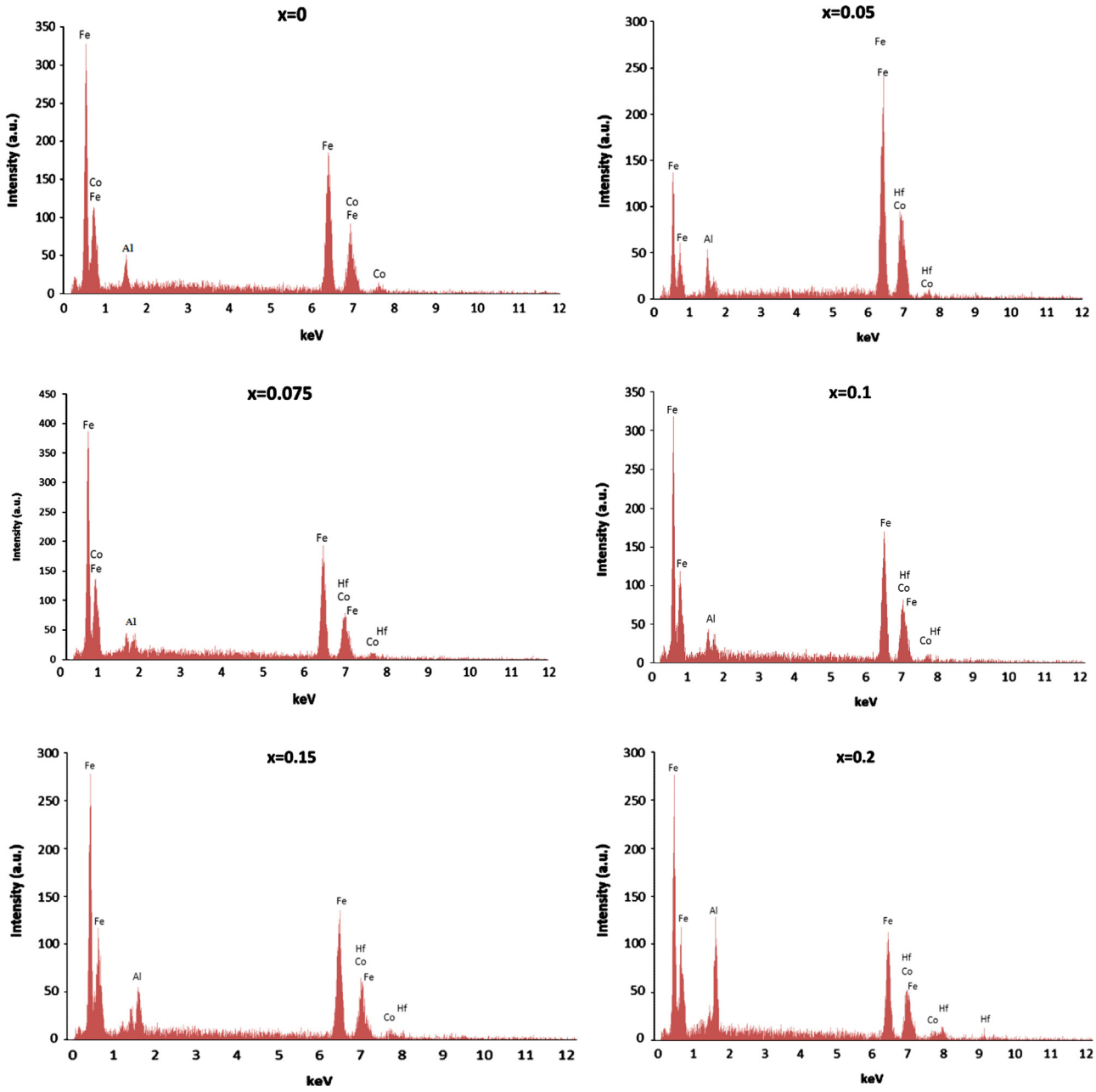

Fig. 5. EDS data of $CoFe_{2-x}Hf_xO_4$ ceramics as a function of x. The peaks due to various elements and their respective energy positions are as indicated.

to 0.20 (Fig. 7). Similarly, α values obtained to increase from 0.59 to 68 with increasing Hf concentration from $x=0.05$ to 0.20. The existence of inertia to the charge movement would cause relaxation of the polarization. It must be emphasized that the τ values are much higher for Hf substituted Co ferrites when compared to that of pure Co ferrite. The increased bond length and lattice constant in Hf doped Co ferrites is evident from structural studies. Therefore, compared to pure Co ferrite, inclusion of larger Hf ions leads to an increase in interionic distance, which in turn increases the hopping distance. This causes the mean relaxation time and spreading factor to increase in Hf doped Co ferrites. Such behavior was also noted in rare-earth ion doped Co- or Ni-based ferrites [5–7,34,45–47]. Specifically, for the case of Co-ferrite, it has been reported that the incorporation of rare-earth ions such as La, Dy, and Gd induces lattice strain coupled with electrical resistivity and dielectric constant enhancement [7,26,34,35].

The frequency variation of $\tan\delta$ is shown in Fig. 8. It is evident that the dielectric loss decreases initially with frequency and a resonance peak is observed at 800 Hz for pure Co ferrite. The resonance takes place when jumping frequency of the localized charge carriers becomes approximately equal to that of the applied AC field. The resonance peak is seen to shift toward high frequency (5 kHz) with increasing Hf concentration. Dielectric loss arises if the polarization lags behind the applied alternating field and is caused by the presence of the secondary phase HfO_2 (impurity phase). The low dielectric loss obtained in the present case is attributed to more structurally perfect and

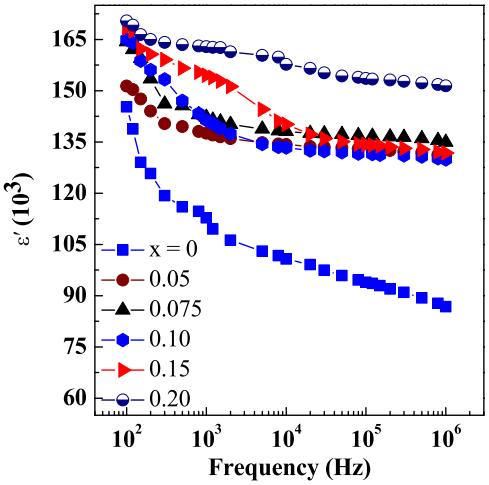

Fig. 6. The dielectric constant dispersion profiles of $CoFe_{2-x}Hf_xO_4$ ceramics. The dielectric constant measured for Hf incorporated cobalt ferrite is always higher than that of pure cobalt ferrite. The dielectric constant increases with x in $CoFe_{2-x}Hf_xO_4$. The dispersion behavior fits (solid lines) to the modified Debye's function (see text).

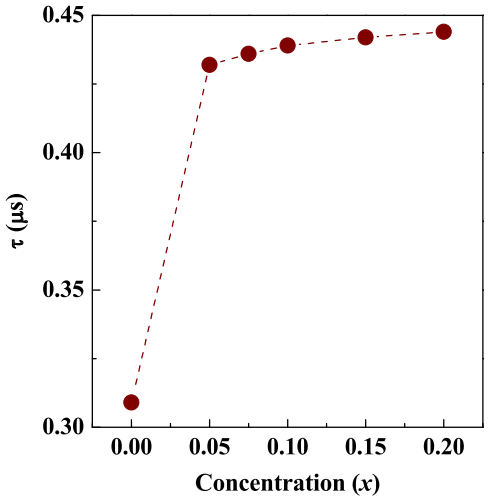

Fig. 7. Variation of relaxation time in $CoFe_{2-x}Hf_xO_4$ ceramics.

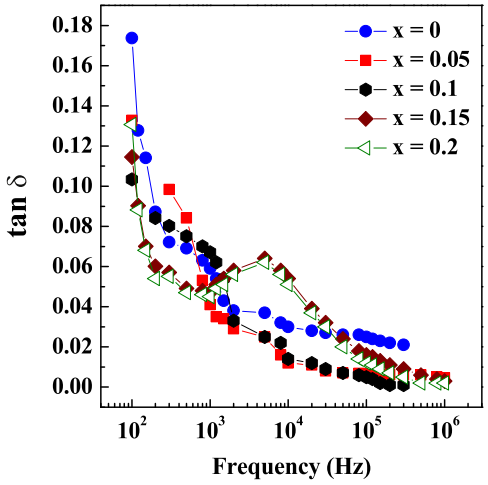

Fig. 8. The frequency variation of dielectric loss factor (tan δ) of $CoFe_{2-x}Hf_xO_4$ ceramics. The data shown are for various x values.

homogeneous sample, which in turn depend on the composition and sintering temperature of the samples.

Finally, based on the observed results in the present work and coupled with the available reports in the literature, a simple model can be discussed to account for the observed changes in the structure and dielectric properties of Co-ferrite ceramics upon metal ion incorporation. It is widely accepted that the inclusion of a metal with larger ionic radius in the spinel lattice will significantly affects the microstructure, magnetic, electrical and dielectric properties of ferrite materials [5–7,34,45–47]. Most importantly, lattice expansion or lattice strain coupled with cation distribution in the lattice is seen to strongly influence the values of electrical resistivity, coercive field, magnetization, magnetostrictive coefficient, and dielectric constant of Co ferrites [5–7,34,45–47]. Recently, we observed increased values of the electrical resistivity in La-doped Co-ferrite, which is attributed to the larger ionic size of La, which induces lattice expansion and resistivity increase [34]. Similarly, it has been reported that the La-incorporated Co-ferrites exhibit the improved structural, magnetic and dielectric properties for the samples prepared by co-precipitation method [46]. From the analysis, it is obvious that the larger metal-ion-incorporation into Co ferrite induces lattice expansion and strain, which depends on the amount of the ionic size and amount incorporated. The increase in real part of the dielectric constant with metal ion incorporation, then, can be explained by the atomic polarizability which is due to the non-centrosymmetry of the doped-ferrite where the distance between the cations in the spinel are larger. In addition, most of these metal ions form the secondary phase which is responsible for the charge accumulation at grain boundaries contributing to the interfacial polarization as we reported previously [5,34]. Most recently, Dascalu et al. successfully adopted our proposed mechanism to account for the observed behavior of La-, Dy- and Gd-incorporated Co-ferrites in their work although the porosity in the samples and specific microstructure details can influence the extent of improvement in either electrical or magnetic or dielectric properties [47].

4. Conclusions

The crystal structure, surface morphology, chemical composition and dielectric properties of Hf-incorporated cobalt ferrite ($CoFe_2O_4$) are investigated. $CoFe_{2-x}Hf_xO_4$ ceramic materials crystallize in inverse spinel phase similar to that of pure $CoFe_2O_4$. Hafnium-induced changes in the crystal structure are significant; lattice expansion in terms of increased lattice constant from 8.374 Å for pure $CoFe_2O_4$ to 8.391 Å for the highest Hf concentration ($x=0.2$) in $CoFe_{2-x}Hf_xO_4$ is noted. Coupled with lattice expansion, dielectric constant of $CoFe_{2-x}Hf_xO_4$ ceramics is also enhanced in progressive manner as a function of x values. Improved dielectric

properties of $CoFe_{2-x}Hf_xO_4$ ceramics compared to pure $CoFe_2O_4$ is attributed to the lattice distortion due to larger Hf-ions substituting for smaller Fe-ions associated structural changes with increased Hf concentration. Frequency variation of the dielectric constant can be modeled with a modified Debye's function, which considers the possibility of more than one ion, contributing to the relaxation. The relaxation time values are much higher for Hf incorporated Co ferrite when compared to that of pure Co ferrite. The proposed mechanism was based on the inclusion of larger Hf ions leading increased cationic distance, which in turn increases the hopping distance, leading to increased mean relaxation time and spreading factor in $CoFe_{2-x}Hf_xO_4$ ceramics.

Acknowledgments

The authors acknowledge with pleasure the support of the Air Force Research Laboratory (Contract number: FA8650-05-D-5039) to perform this research work.

References

[1] A. Rafferty, T. Prescott, D. Brabazon, Sintering behavior of cobalt ferrite ceramic, Ceramics International 34 (2008) 15–21.
[2] R.C. Che, C.Y. Zhi, C.Y. Liang, X.G. Zhou, Fabrication and microwave absorpotion of carbon nanotubes/$CoFe_2O_4$ spinel nanocomposite, Applied Physics Letters 88 (2006) 033105-1–033105-3.
[3] H. Yüngevis, E. Ozel, Effect of milling process on the properties of $CoFe_2O_4$, Ceramics International 39 (2013) 5503–5511.
[4] M. Sugimoto, The past, present and future of ferrites, Journal of the American Ceramic Society 82 (1999) 269–280.
[5] K. Kamala Bharathi, G. Markendeyulu, C.V. Ramana, Structural, magnetic, electrical, and magnetoelectric properties of Sm- and Ho-substituted nickel ferrites, Journal of Physical Chemistry C 115 (2011) 554–560.
[6] K. Kamala Bharathi, M. Noor-A-Alam, R.S. Vemuri, C.V. Ramana, Correlation between microstructure, electrical and optical properties of nanocrystalline $NiFe_{1.925}Dy_{0.075}O_4$ thin films, RSC Advances 2 (2012) 941–948.
[7] K. Kamala Bharathi, G. Markendeyulu, C.V. Ramana, Enhanced dielectric property of Ni ferrite by Sm and Ho substitution, Electrochemical and Solid-State Letters 13 (2010) G98–G102.
[8] Z. Gu, X. Xiang, G. Fan, F. Li, Facile synthesis and characterization of cobalt ferrite nanocrystal via a simple reduction–oxidation route, Journal of Physical Chemistry C 112 (2008) 18459–18466.
[9] U. Kurtan, R. Topkaya, A. Baykal, M.S. Toprak, Temperature dependent magnetic properties of $CoFe_2O_4$/CTAB nanocomposite synthesized by sol–gel auto-combustion method, Ceramics International 39 (2013) 6551–6558.
[10] R. Peelamedu, C. Grimes, D. Agrawal, R. Roy, P. Yadoji, Ultralow dielectric constant nickel–zinc ferrites using microwave sintering, Journal of Materials Research 18 (2003) 2292–2295.
[11] F. Vereda, J. Vicente, R. Hidalgo-Álvarez, Synthesis of Ni ferrite and Co ferrite rodlike particles by superposition of a constant magnetic field, Journal of Materials Research 23 (2008) 1764–1775.
[12] F. Cheng, C. Liao, J. Kuang, Z. Xu, C. Yan, L. Chen, H. Zhao, Z. Liu, Nanostructure magneto-optical thin films of rare earth (RE=Gd,Tb,Dy) doped cobalt spinel by sol–gel synthesis, Journal of Applied Physics 85 (1999) 2782-1–2782-5.
[13] W. Eerenstein, N.D. Mathur, J.F. Scott, Multiferroic and magnetoelectric materials, Nature 442 (2006) 759–765.
[14] D.I. Khomskii, Multiferroics: different ways to combine magnetism and ferroelectricity, Journal of Magnetism and Magnetic Materials 306 (2006) 1–8.
[15] N.A. Hill, Why are there so few magnetic ferroelectrics?, Journal of Physical Chemistry B 104 (2000) 6694–6709
[16] X.L. Zhong, M. Liao, J.B. Wang, S.H. XieY, C. Zhou, Structural, ferroelectric, ferromagnetic, and magnetoelectric properties of the lead-free $Bi_{3.15}Nd_{0.85}Ti_3O_{12}$/$CoFe_2O_4$ double-layered thin film, Journal of Crystal Growth 310 (2008) 2995–2998.
[17] M. Fiebig, Revival of magnetoelectric effect, Journal of Physics D: Applied Physics 38 (2005) R123–R152.
[18] S.L. Kadam, C.M. Kanamadi, K.K. Patankar, B.K. Chougule, Dielectric behaviour and magnetoelectric effect in $Ni_{0.5}Co_{0.5}Fe_2O_4$+$Ba_{0.8}Pb_{0.2}TiO_3$ ME composites, Materials Letters 59 (2005) 215–219.
[19] E. Manova, B. Kunev, D. Paneva, I. Mitov, L. Petrov, Mechano-synthesis, characterization, and magnetic properties of nanoparticles of cobalt ferrite, $CoFe_2O_4$, Chemistry of Materials 16 (2005) 5689–5696.
[20] Q. Song, Z.J. Zhang, Correlation between spin–orbital coupling and the superparamagnetic properties in magnetite and cobalt ferrite spinel nanocrystals, Journal of Physical Chemistry B 110 (2006) 11205–11209.
[21] I.H. Gul, A. Maqsood, Structural, magnetic and electrical properties of cobalt ferrites prepared by the sol–gel route, Journal of Alloys and Compounds 465 (2008) 227–231.
[22] C.V. Gopal Reddy, S.V. Manorama, V.J. Rao, Semiconducting gas sensor for chlorine based on inverse spinel nickel ferrite, Sensors and Actuators B 55 (1990) 90–95.
[23] J.L. Gunjakar, A.M. More, V.R. Shinde, C.D. Lokhande, Synthesis of nanocrystalline nickel ferrite ($NiFe_2O_4$) thin films using low temperature modified chemical method, Journal of Alloys and Compounds 465 (2008) 468–473.
[24] Y.N. Nuli, Q.Z. Qin, Nanocrystalline transition metal ferrite thin films prepared by an electrochemical route for Li-ion batteries, Journal of Power Sources 142 (2005) 292–297.
[25] G.L. Sun, J.B. Li, J.J. Sun, X.Z. Yang, The influences of Zn^{2+} and some rare-earth ions on the magnetic properties of nickel–zinc ferrites, Journal of Magnetism and Magnetic Materials 281 (2004) 173–177.
[26] N. Rezlescu, E. Rezlescu, C. Pasnicu, M.L. Craus, Effects of the rare-earth ions on some properties of nickel–zinc ferrite, Journal of Physics: Condensed Matter 6 (1994) 5707–5716.
[27] R. Hochschild, H. Fuess, Rare-earth doping of nickel zinc ferrites, Journal of Materials Chemistry 10 (2000) 539–542.
[28] E.E. Sileo, E. Silvia, E. Jacobo, Gadolinium–nickel ferrites prepared from metal citrates precursors, Physica B 354 (2004) 241–245.
[29] M. Ajmal, A. Maqsood, Influence of zinc substitution on structural and electrical properties of $Ni_{1-x}Zn_xFe_2O_4$ ferrites, Materials Science and Engineering B 139 (2007) 164–170.
[30] J.J. Yuan, Q. Zhao, Y.S. Xu, Z.G. Liu, X.B. Du, G.H. Wen, Synthesis and magnetic properties of $CoFe_2O_4$ nanowire arrays, Journal of Magnetism and Magnetic Materials 321 (2009) 2795–2798.
[31] S. Amiri, H. Shokrollahi, The role of cobalt ferrite magnetic nanoparticles in medicine, Materials Science and Engineering C 33 (2013) 1–8.
[32] S. Chikazumi, Physics of Ferromagnetism, Oxford University Press, New York, 1997.
[33] J. Smith, H.P.J. Wijn, Ferrites, Philips Technical Library, Eindhoven, Holland, 1965.
[34] K. Kamala Bharathi, C.V. Ramana, Improved dielectric properties La-doped Co ferrite, Journal of Materials Research 26 (2011) 584–591.
[35] R.S. Devan, Y.D. Kolekar, B.K. Chougule, Effect of cobalt substitution on the properties of nickel–copper ferrite, Journal of Physics: Condensed Matter 18 (2006) 9809–9822.
[36] M. Noor-A-Alam, C.V. Ramana, Synthesis and microstructure of Gd_2O_3-doped HfO_2 ceramics, Ceramics International 38 (2012) 1801–1806.
[37] M. Noor-A-Alam, C.V. Ramana, Structure and thermal conductivity of yttria-stabilized hafnia ceramic coatings grown on nickel-based alloy, Ceramics International 38 (2012) 2957–2961.
[38] J. Robertson, High dielectric constant gate oxides for metal oxide Si transistors, Reports on Progress in Physics 69 (2006) 327–396.
[39] G.D. Wilk, R.M. Wallace, J.M. Anthony, High-κ gate dielectrics: current status and materials properties considerations, Journal of Applied Physics 89 (2001) 5243-1–5243-33.

[40] C.V. Ramana, K. Kamala Bharathi, A. Garcia, A.L. Campbell, Growth behavior, lattice expansion, strain and surface morphology of nanocrystalline, monoclinic HfO_2 thin films, Journal of Physical Chemistry C 116 (2012) 9955–9960.

[41] C.V. Ramana, A. Ait-Salah, S. Utsunomiya, J.F. Morhange, A. Maugher, F. Gendron, C.M. Julien, Spectroscopic and chemical imaging analysis of Lithium Iron triphosphate, Journal of Physical Chemistry C 111 (2007) 1049–1054.

[42] C.V. Ramana, A. Ait-Salah, S. Utsunomiya, U. Becker, A. Mauger, F. Gendron, C.M. Julien, Structural characteristics of Nickel phospahtes studied using analytical electron microscopy and Raman spectroscopy, Chemistry of Materials 18 (2006) 3788–3794.

[43] K.S. Cole, R.H. Cole, Dispersion and absorption in dielectrics I. Alternating current characteristics, Journal of Chemical Physics 9 (1941) 341–351.

[44] J.C. Anderson, Dielectrics, Spottiswoode, Ballantyne & Co Ltd, London and Colchester, 1964.

[45] K. Kamala Bharathi, G. Markendeyulu, C.V. Ramana, Microstructure, AC electrical conductivity and DC electrical characteristics of $NiFe_{2-x}Gd_xO4$ ($x=0$, 0.05, 0.075), AIP Advances 2 (2012) 012139.

[46] Pawan Kumar, S.K. Sharma, M. Knobel, M. Singh, Effect of La^{3+} on the electric, dielectric and magnetic properties of cobalt ferrite processed by co-precipitation technique, Journal of Alloys and Compounds 508 (2010) 115–118.

[47] D. Dascalu, T. Popescu, M. Feder, O.F. Caltun, Structural, electric and magnetic properties of $CoFe_{1.8}RE_{0.2}O_4$ (RE=Dy, Gd, La) bulk materials, Journal of Magnetism and Magnetic Materials 333 (2013) 69–74.